Cardiovascular Engineering and Technology (© 2018)
https://doi.org/10.1007/s13239-018-0352-3

The Mechanical Characterisation of Bovine Embolus Analogues Under Various Loading Conditions

F. Malone,[1] E. McCarthy,[1] P. Delassus,[1] P. Fahy,[1] J. Kennedy,[2,3] A. J. Fagan,[4,5] and L. Morris[1]

[1]GMedTech, Department of Mechanical and Industrial Engineering, Galway-Mayo Institute of Technology, Galway, Ireland; [2]Materials Research Institute, Athlone Institute of Technology, Athlone, Co. Westmeath, Ireland; [3]Kastus Technologies, Grangegorman, Dublin 7, Ireland; [4]National Centre for Advanced Medical Imaging, St. James's Hospital/School of Medicine, Trinity College Dublin, Dublin, Ireland; and [5]Department of Radiology, Mayo Clinic, Rochester, MN 55905, USA

(Received 4 October 2016; accepted 22 March 2018)

Associate Editors Ulrich Steinseifer and Ajit P. Yoganathan oversaw the review of this article.

Abstract—Embolus Analogues (EAs) can provide understanding of the mechanical characteristics of blood clots of cardiac origin. Bovine EAs ($n = 29$) were fabricated with varying concentrations of thrombin (0–20 NIHU/ml blood). Histological staining confirmed that EA composition compared sufficiently with human samples reported in literature. EAs were mechanically described under seven testing conditions: tensile, compression, shear wave ultrasound elastography (SWE), parallel plate rheometry, indentation, creep and relaxation. The Young modulus of bovine EAs in tension varied from 7 kPa (5% strain) to 84 kPa (50% strain). The compressive Young modulus increased with increasing thrombin concentration, which was in agreement with the SWE results. There was no significant difference in Young modulus throughout the clot ($p < 0.05$). The EAs displayed a non-linear response under parallel plate rheometry, creep and stress relaxation. The 3rd order Mooney–Rivlin constitutive equation and Standard Linear Solid model were used to fit the non-linear stress–strain response and time-dependent properties, respectively. This is the first study in which bovine EAs, with and without addition of thrombin, are histologically and mechanically described with corresponding proposed constitutive equations. The equations and experimental data determined can be applied for future numerical and experimental testing of mammalian EAs and cardiac source clots.

Keywords—Embolus analogues, Mechanical testing, Blood clots, Cardiac source clots, Constitutive equations.

INTRODUCTION

Worldwide, 15 million people suffer a stroke each year with approximately one-third of these strokes being fatal. Ischemic stroke accounts for > 80% of all strokes in Europe and North America and > 70% in the Far East.[19] Acute ischaemic stroke (AIS) results from a sudden occlusion of a major cerebral artery. 15–20% of these occlusions occur when a blood clot that has originated from a cardiac source embolises and lodges itself within the cerebral vasculature and prevents brain tissue perfusion.[18] An increased stress response, stasis, dehydration and inflammatory processes associated with surgery and critical illness further increase the chances of thrombus formation in the heart or vascular tree.[20]

Atrial fibrillation (AF) is a major contributor to blood clot formation within the heart and is responsible for 45% of all embolic strokes.[1] During AF, stasis of blood in the left atrium predisposes to clot formation within the left atrial appendage. These thrombi can range in size from a few millimetres to 4 cm and are found in 5–14% of patients with AF symptoms lasting more than two days.[24] Thus AF is becoming the most common source of arterial emboli and increases an individual's risk of stroke fourfold on average.[4] This risk increases with age, where AF is the direct cause of 1 in 4 strokes in patients > 80 years old.[10,13,25]

Trans-catheter Aortic-Valve Implantation (TAVI) is another high risk factor associated with stroke epidemiology.[24] TAVI represents a novel treatment option for inoperable or high surgical risk patients with severe symptomatic aortic valve disease. Stroke may occur after TAVI as a result from embolization from the valve during balloon valvuloplasty and valve deployment or embolisation of aortic atheroma during device passage. A meta-analysis of 10,037 cases treated with TAVI reported stroke/TIA rates after 30 days

Address correspondence to L. Morris, GMedTech, Department of Mechanical and Industrial Engineering, Galway-Mayo Institute of Technology, Galway, Ireland. Electronic mail: fiona.malone@research.gmit.ie, liam.morris@gmit.ie

Published online: 27 March 2018

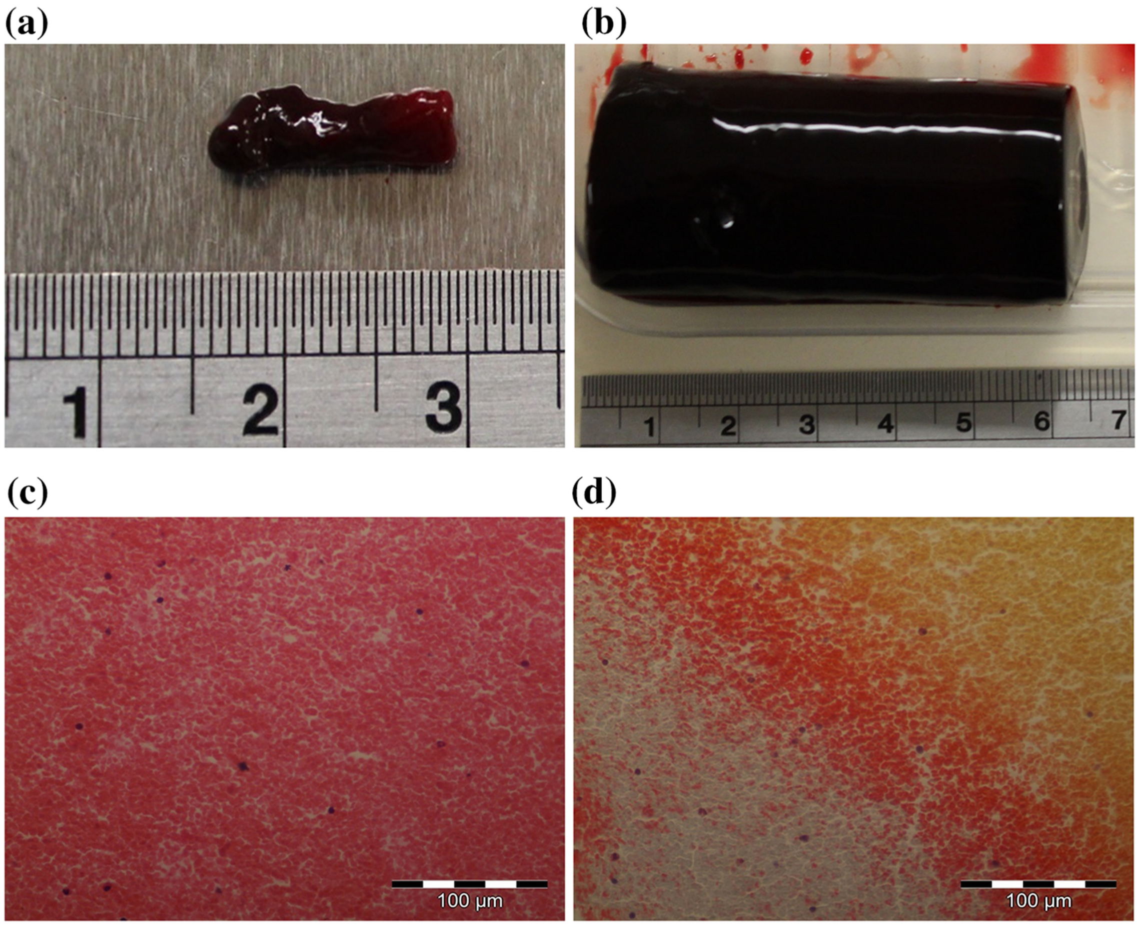

FIGURE 1. (a) and (b) Thrombin induced bovine EAs (5NIH units/ml of blood); (c) EA section stained using H & E; (d) EA section stained using MSB (C and D images × 40 magnification).

post-implantation of 3.3 ± 1.8% (range 0–6%).[9] Most of these strokes were major strokes and were associated with increased mortality within in the first 30 days.

Cardiac source blood clots, at the macro level, are viscoelastic, gel-like materials that consist of a vast amount of liquid. Chueh *et al.* performed compression tests on thromboemboli retrieved from clinical cases. However, the retrieval of thrombi from humans for the investigation of AIS is expensive, complicated, time-consuming and highly regulated. Embolus analogues (EAs) have played a unique role in understanding the pathophysiology, morphology and mechanical characteristics of thrombi underlying vascular occlusion in acute ischemic stroke. Other researchers have performed a range of mechanical tests on coagulated EAs extracted from humans and animals under tensile,[6] compression,[6,8,21,26] elastography[3,27,29] and rheometry.[5] Few studies quantified the EA's viscoelastic properties dynamically by compression[29] and elastography.[27]

To date, EAs fabricated from mammalian blood within the same study have not been subjected to a broad range of mechanical test methods, nor have any constitutive equations been proposed for tensile, compression or time-dependent testing. The determination of the nonlinear mechanical characteristics of the blood clots can be applied to future computational studies and the development of synthetic clot replicas, which can inform the design of clot retrieval devices. The aim of this study was to assess the mechanical properties of bovine EAs under a variety of loading conditions (tensile, compression, shear, indentation and time dependent) with formulated constitutive equations. Knowledge of these properties is critical for determining the clot trajectory and lodgement location of emboli originating from a cardiac source.

MATERIALS AND METHODS

Clot Fabrication

Bovine blood from six animals was obtained from a local abattoir (Burkes, Gort, Galway, Ireland) which is an EU approved abattoir supervised by Galway County Council veterinary services. Bovine blood is

TABLE 1. Mechanical tests carried out on bovine blood from six animals.

	Loading conditions applied to sample						
Animal	Tensile	Shear wave elastography	Compression	Indentation	Parallel plate rheometry	Creep	Stress relaxation
A1					✔		
A2			✔		✔		
A3			✔				
A4			✔	✔		✔	
A5	✔	✔	✔				✔
A6	✔				✔		

recognised as a suitable source for the creation of mammalian EAs.[21] EAs ($n = 29$) were produced by two techniques: (1) allowing the blood to coagulate in a static environment and (2) promoting the coagulation processes by adding bovine thrombin (Sigma Aldrich, Dublin, Ireland) ranging in concentrations from 5 to 20 NIH units of thrombin/ml of blood.[12] The clotting process took approximately 1–2 h, as shown in Figs. 1a and 1b for a small and large sized clot, respectively. Table 1 shows the range of mechanical tests carried out on the blood clot samples.

Histological Analysis

Clot samples were fixed and processed using RVG/1 Histology Tissue Processor (Intelsint) and embedded in paraffin wax. The samples were sectioned to thicknesses between 3 and 5 μm and stained using Haematoxylin and Eosin (H & E) and Martius Scarlet Blue (MSB). The stained sections were examined microscopically using the Olympus BX41 microscope (Olympus America Inc., USA), and digital images were obtained using the Olympus camera. H & E stains nuclei purple and erythrocytes red. It non-specifically stains cytoplasm and extracellular matrix in varying shades of pink (Fig. 1c). MSB provides distinct recognition of fibrin, staining the areas red and erythrocytes yellow (Fig. 1d). The manufactured EAs exhibit components histologically similar to human thrombi retrieved from stroke patients and manufactured mammalian EAs.[6,17,21] The presence of platelets was not histologically confirmed.

Uniaxial Tensile Tests

The stress–strain response in uniaxial tension was found by the Instron 5544 (Instron 5500 series, MA, USA) using a 10 N load cell, with clot motion monitored using a couple charged device (CCD) camera with a frame rate of 50 Hz and a resolution of 12 MPixels. Bovine blood with varying levels of thrombin (1 day old, both samples from Animal 5 and 6 induced with 20 NIHU and 10 NIHU, respectively), was coagulated into an acetal mould, forming a cylindrical dogbone shape (Fig. 2a). The cylindrical dogbone shape was based on the ASTMD-412-D standard and is similar in shape to the samples of unknown dimension, as tested by Krasokha *et al.*[21] Sandpaper was used to grip the clot within the clamps, to prevent slippage (Fig. 2b). The samples were tested cyclically to a maximum extension of 10% with 10 cycles at a displacement rate of 2 mm/s and then pulled to failure. Upon completion of the test, an open source tracking software Kinovea (Kinovea, Version 0.8.15) was used to track selected pixels along the sample, eliminating the effects of slippage at the clamp jaws. The software automatically tracks the selected pixel based on its grey scale value which does not change during the test within the displacement range. The pixel displacements were automatically exported to an Excel file.

Compression Tests

The stress–strain response in compression was found using the same Instron and CCD camera as described for the tensile testing. Bovine blood with varying thrombin concentrations of 0, 5, and 10 NIHU/ml blood were coagulated (2 days old) in a vial of inner diameter of 30 mm and height of 15–20 mm (Fig. 2e). This height to diameter ratio prevented the sample from buckling during compression testing. Figure 2f shows a sample under compression using a 50 mm diameter plunger. The displacement rate was 0.25 mm/s similar to Krasokha *et al.*[21] Compression tests were conducted on clot samples from 4 animals (Animals 2-5) with no addition of thrombin ($n = 7$). The effects of thrombin concentration was assessed for two animals (Animal 3 and 5; $n = 6$). Three varying displacement rates of 0.25, 0.5 and 1 mm/s were conducted to assess rate dependency ($n = 3$).

Ultrasound Shear Wave Elastography (SWE)

Ultrasound SWE is another technique capable of measuring the stiffness of biological tissues.[28] Nonlinear elastic properties have been obtained by SWE

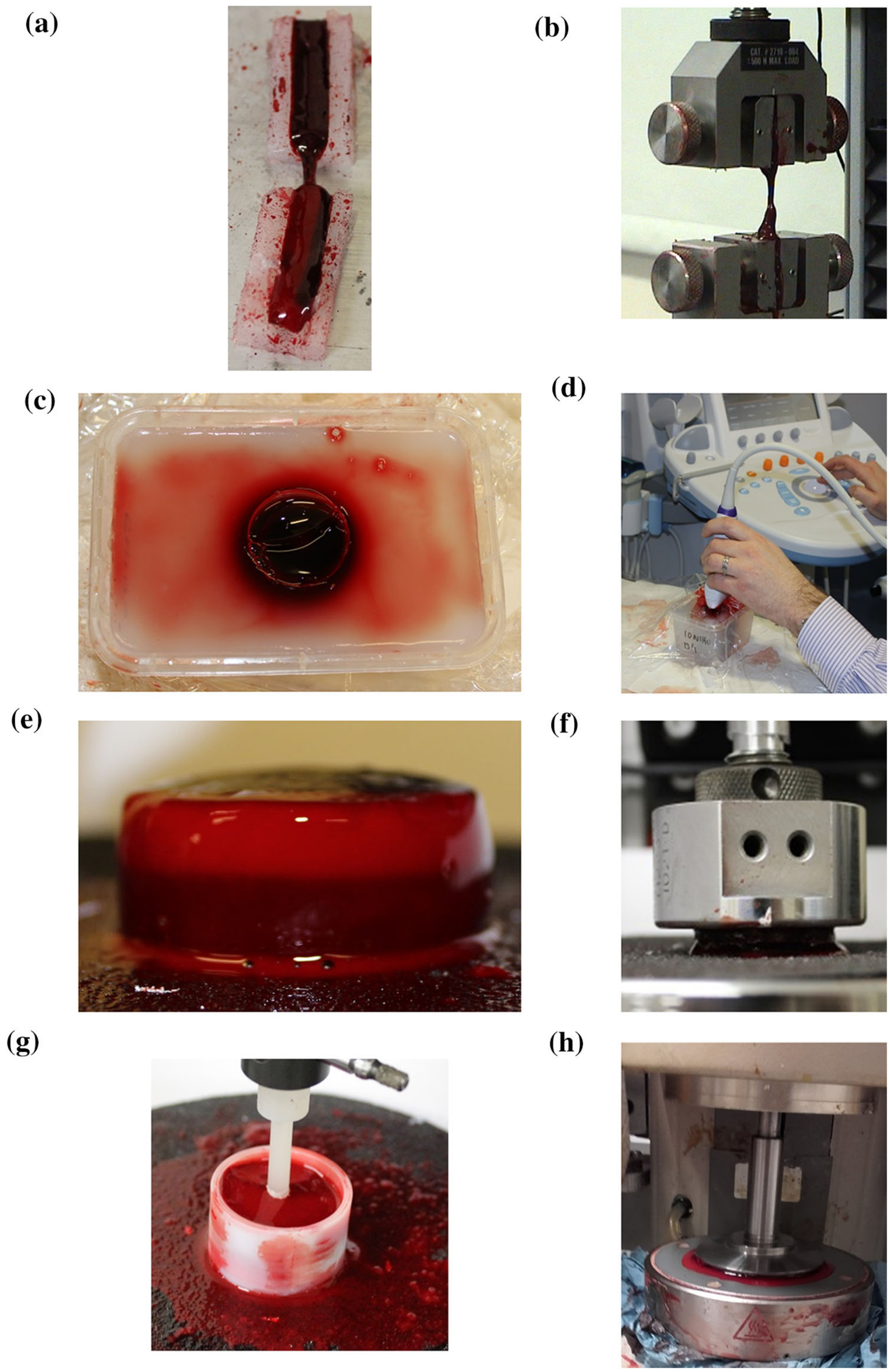

FIGURE 2. **(a) Cylindrical dogbone EA specimen; (b) Clamped dogbone EA specimen under tensile loading; (c) Cylindrical specimen positioned within agar; (d) cylindrical specimen positioned within agar under ultrasound shear wave eleastography testing; (e) Cylindrical EA specimen for compression, indentation, dynamic rheometry, creep and stress relaxation testing; (f) Cylindrical EA specimen under compression testing; (g) Cylindrical EA specimen positioned within a rigid cylindrical housing for indentation testing; (h) Cylindrical EA specimen under dynamic rheometry testing.**

for describing brain tissue,[15] breast tissue[2] and agar-gelatin/poly vinyl alcohol based phantoms.[11] Here, SWE was performed to measure the initial Young modulus and not the non-linear elastic properties on 4 bovine EAs (2 days old, Animal 5) and tested with thrombin concentrations of 0, 5, 10 and 20 NIHU units/ml blood, using an Aixplorer scanner (Supersonic Imagine, France) at an imaging frequency of 6 MHz. A cylindrical sample of height 40 mm and diameter 30 mm was positioned within agar (Fig. 2c). SWE applies a time-varying acoustic force to the tissue *via* an ultrasonic probe to generate shear waves. The shear wave velocity (c) is measured using conventional longitudinal-wave ultrasound imaging techniques and in terms of the shear modulus (G) is found by:

$$c = \sqrt{\frac{G}{\rho}} \tag{1}$$

where ρ is the blood clot density.

The relationship between Young Modulus (E) and the shear modulus (G) is given by:

$$E = 2(v + 1)G \tag{2}$$

Assuming a Poisson ratio of near 0.5, which is valid for a high water content medium such as blood clots, E = 3G. Therefore, the initial Young Modulus (E) can be found by:

$$E = 3\rho c^2 \tag{3}$$

The depth of the sample facilitated accurate measurements and excluded the effects of the probe's compression at the clot and probe interface (Fig. 2d). Positioning the EAs within agar prevented undesirable sample container boundary reflections from occurring that would otherwise have interfered with the measuring process. The samples' elastic moduli were measured in circular regions of interest which were carefully positioned within the region of the clot by an experienced user (AF) to ensure no contribution from the surrounding agar. The large sample dimension allows for the ultrasound to penetrate the sample fully, minimising the elastic contribution of the agar. The Young modulus was found within the selected region of interest, which was a sufficient distance away from the surrounding agar.

Indentation

A series of indentation tests at 0.5 mm/s were performed using a 5 mm diameter cylindrical flat punch tip (2 days old, Animal 4). The load–displacement response was found using the same procedure as used for the tensile and compression tests. An indentation of 1 mm was chosen so as not to pierce the clot samples. Five indentations were performed on the top and bottom of one clot sample (Animal 4). The sample was positioned within a rigid cylindrical housing (Fig. 2g).

Dynamic Rheometry

Dynamic shear rheometry was used to find the torsional shear loss and storage moduli using the AR 1000 rheometer with 50 mm diameter plunger (TA Instruments, DE, USA). The storage and loss moduli were found by applying a sinusoidal strain sweep on five EAs (Animal 1, 2 and 6), of different thrombin concentrations (Fig. 2h, 2 days old, 0, 5, and 10 NIHU/ml blood), at a frequency of 1 Hz until failure.

The storage (G') and loss (G'') moduli in shear are represented by the complex shear modulus G^* by:

$$G^* = G' + iG'' \tag{4}$$

where

$$G' = G^* \cos\delta \tag{5}$$

$$G'' = G^* \sin\delta \tag{6}$$

and the phase angle (δ) is found by:

$$\tan\delta = \frac{G''}{G'} \tag{7}$$

The absolute shear modulus $|G^*|$ is given by:

$$|G^*| = \sqrt{G'^2 + G''^2} \tag{8}$$

The storage and loss moduli were found by applying a sinusoidal strain sweep on five EAs (Animal 1, 2 and 6), of different thrombin concentrations (Fig. 2h, 2 days old, 0, 5, and 10 NIHU/ml blood), at a frequency of 1 Hz until failure.

Creep and Stress Relaxation

Creep and stress relaxation tests of 3 loads (0.3, 1, 2 N) and 3 displacements (1, 2, 4 mm), respectively, were performed in compression on two clot samples (Animal 4 and 5, 1 day old) with no added thrombin for a period of 1 h per test. The dimension of the clot samples were the same as those used for the compression testing (Fig. 2e).

Constitutive Modelling

All clots samples were modelled as isotropic and incompressible. The Mooney–Rivlin third order hyperelastic strain energy density function model was applied to the non-linear stress response. The third order Mooney–Rivlin strain energy density function (W) is given by Eq. (2)[22]:

$$W = a_{10}(I_1 - 3) + a_{01}(I_2 - 3) + a_{11}(I_1 - 3)(I_2 - 3) + a_{20}(I_1 - 3)^2 + a_{30}(I_1 - 3)^3 \quad (9)$$

where I_1 and I_2 are the first and second principal strain invariants and the a-values are the hyper-elastic constants. The 1st and 2nd invariants are given in terms of the principle stretch ratios λ_1, λ_2 and λ_3:

$$I_1 = \lambda_1^2 + \lambda_2^2 + \lambda_3^2 \quad (10)$$

$$I_2 = \lambda_1^2\lambda_2^2 + \lambda_2^2\lambda_3^2 + \lambda_3^2\lambda_1^2 \quad (11)$$

where, λ_1 is the principal stretch along the loading direction, and λ_2 and λ_3 are the principal stretches along the lateral directions.

For incompressible conditions $\lambda_1\lambda_2\lambda_3 = 1$. Therefore, for uniaxial tension and compression:

$$\lambda_1 = \lambda \quad (12)$$

$$\lambda_2 = \lambda_3 = \lambda^{-1/2} \quad (13)$$

$$\lambda = 1 + \varepsilon \quad (14)$$

where ε is the strain.

Therefore I_1, I_2 and W can be rewritten as:

$$I_1 = \lambda^2 + \frac{2}{\lambda} \quad (15)$$

$$I_2 = 2\lambda + \frac{1}{\lambda^2} \quad (16)$$

$$W = a_{10}\left(\lambda^2 + \frac{2}{\lambda} - 3\right) + a_{01}\left(2\lambda + \frac{1}{\lambda^2} - 3\right) + a_{11}\left(\lambda^2 + \frac{2}{\lambda} - 3\right)\left(2\lambda + \frac{1}{\lambda^2} - 3\right) + a_{20}\left(\lambda^2 + \frac{2}{\lambda} - 3\right)^2 + a_{30}\left(\lambda^2 + \frac{2}{\lambda} - 3\right)^3 \quad (17)$$

The true/Cauchy stress response is given by:

$$T(\lambda) = \lambda\frac{\delta W}{\delta\lambda} \quad (18)$$

The standard linear solid model (SLS) or Zener model was used to fit the creep ($c(t)$) and stress relaxation ($s(t)$) data. The SLS model comprises of a spring with a Young modulus E_1 in series with the Kelvin–Voight model comprising of a spring (Young modulus E_2) in parallel with a dashpot (damping coefficient μ).

$$c(t) = \frac{1}{E_1} + \frac{1}{E_2}\left(1 - e^{-t/\tau_1}\right) \quad (19)$$

$$s(t) = \frac{E_1E_2}{E_1 + E_2}\left(1 + \frac{E_1}{E_2}e^{-t/\tau_2}\right) \quad (20)$$

where the relevant relaxation times are given by

$$\tau_1 = \frac{\mu}{E_2} \text{ and } \tau_2 = \frac{\mu}{E_1 + E_2} \quad (21)$$

The method of least squares was applied to find the coefficients within the constitutive equations, which best fit the experimental data. A series of function files were written in Matlab, minimising $\sum_{i=1}^{n}(y_i - y_{\text{fit}})^2$ by applying the non-linear Newton Iteration method, where y_i is the value of the experimental data on the y-axis and y_{fit} is the value of the constitutive model on the y-axis.

RESULTS

Tensile

Figures 3a and 3b show the tensile results for the dogbone EAs (n = 4). Figure 3a displays the stress–strain response of the samples from 0 to 20% strain. Three out of the four samples either slipped or tore at the jaws beyond 20% strain. Figure 3b displays one clot sample (A6, C1) with 10 NIHU added thrombin dogbone sample to failure, showing two distinct linear regions. Table 2 summarises the Young modulus (slope of linear fit) for all samples tested, with best fit coefficients based on the Mooney–Rivlin Third Order Model for A6, C1 (Fig. 3b). Figures 3c and 3d display the necking and Fig. 3e display the failure that occurred within the 10 NIHU dogbone sample.

Based on a linear fit 0–20% strain, the modulus varied from 14 to 51 kPa. For the one clot (A6, C1), the Young modulus varied from 7 kPa (5% strain) to 84 kPa (40% strain) based on the Mooney–Rivlin Constitutive model.

Compression

Figures 4a–4c shows the stress–strain response in compression results for a range of clot samples ranging from 0 to 10 NIHU thrombin/ml blood. The effect of strain rate is given in Fig. 4d (0 NIHU). Table 3 summarises the best fit coefficient values for the compression samples and corresponding Young modulus in compression based on the Mooney–Rivlin constitutive model.

The compressive Young modulus increases with increasing strain and with increasing thrombin concentration. For samples containing no added throm-

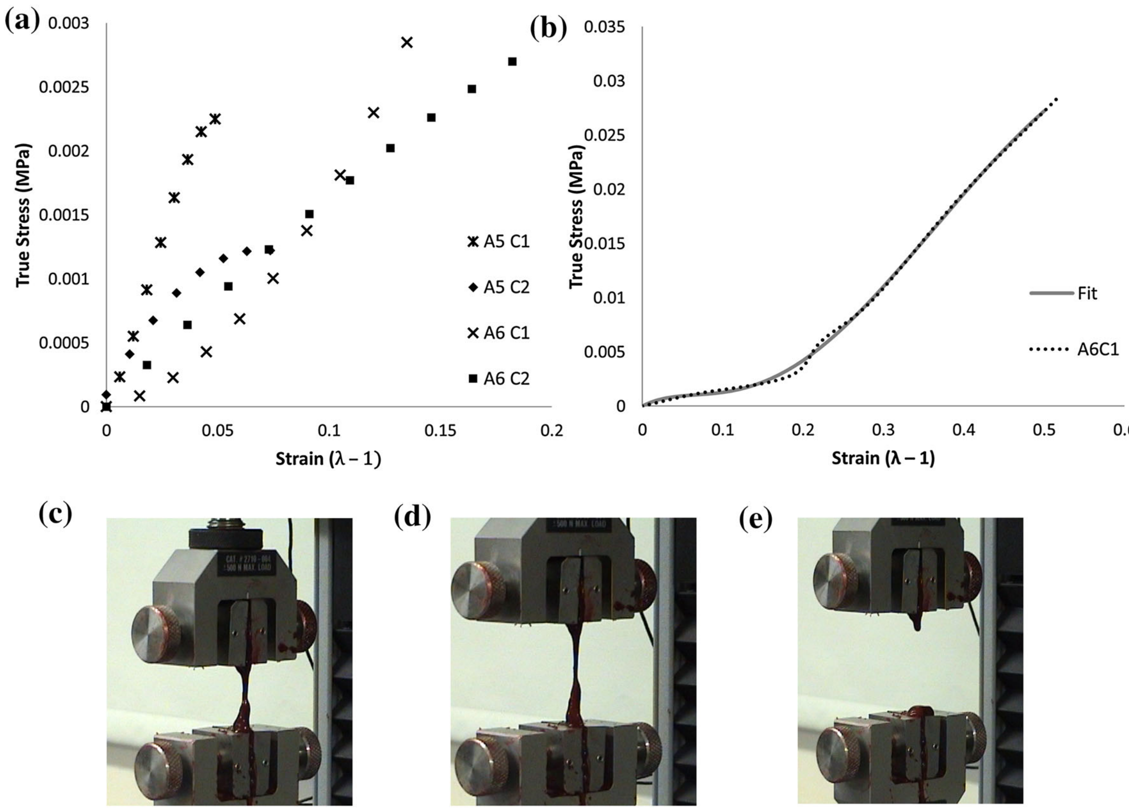

FIGURE 3. (a) Stress–strain results of four dogbone EAs from 0 to 20% strain; (b) Stress–strain response of one dogbone EA (A6C1; 10 NIHU thrombin, Dashed line) with best fit coefficient based on the Mooney–Rivlin Third Order Model (Solid line); (c–e) Specimen A6C1 under tensile testing with necking (d) and failure (e).

TABLE 2. Young modulus in tension for 0–20% strain and fit co-efficients and E values 0–50% strain for A6 C2.

	Clot samples			
	Animal 5 (kPa)		Animal 6 (kPa)	
% strain	C1	C2	C1	C2
0–20	50.5	19.7	21.4	14
Coefficients (kPa)				Animal 6 Clot 1 (kPa)
a10				90.01
a01				96.63
a20				161.3
a11				260.3
a30				9.49
% strain				A6 C1 Young modulus (kPa)
5				6.7
10				10.3
20				50.7
30				81.4
40				83.7
50				65.4

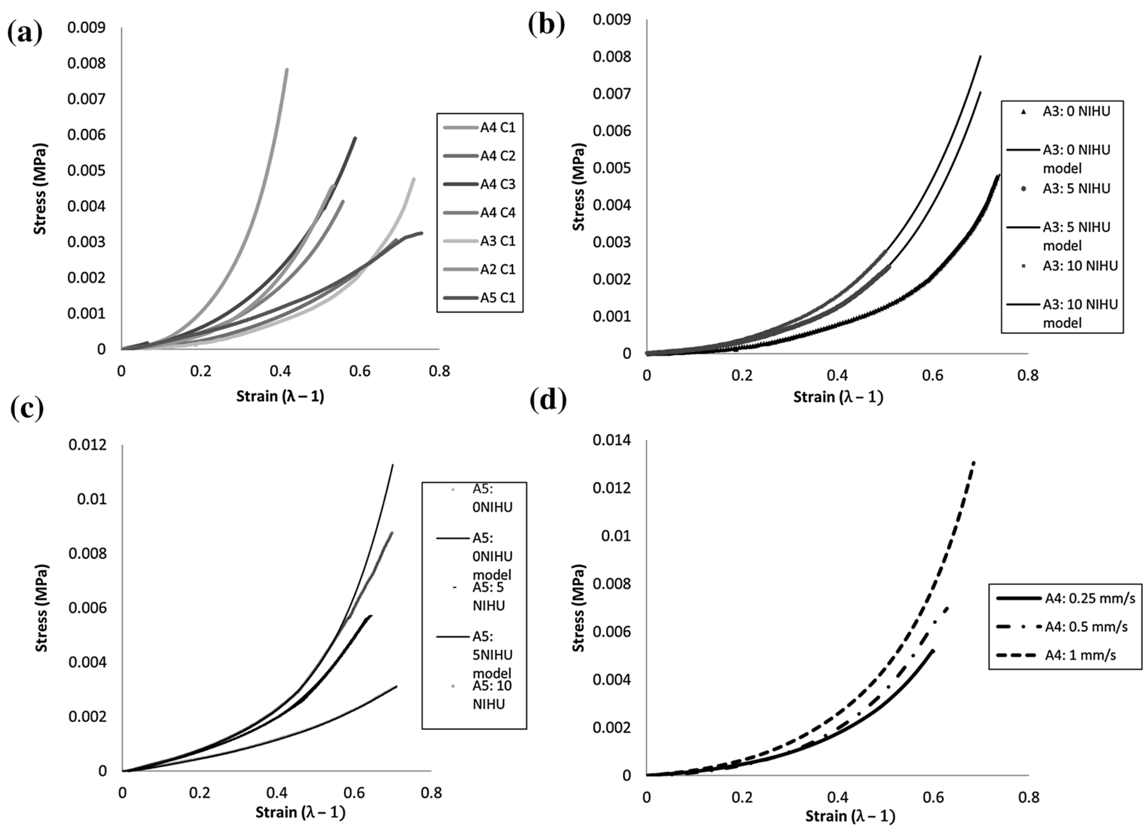

FIGURE 4. (a) Compressive stress–strain response of seven samples from four different animals with no added thrombin; (b) Compressive stress–strain response of three EA samples from same animal (Animal 3, Dashed line) with varying thrombin concentration and model (Solid line); (c) Compressive stress–strain response of three EA samples from same animal (Animal 5, Dashed line) with varying thrombin concentration and model (Solid line); (d) Stress–strain response of three EA samples from same animal (Animal 4) with variation in strain rates.

TABLE 3. Best fit co-efficient and young modulus in compression for the Mooney–Rivlin constitutive model.

	0 NIHU			Animal 3			Animal 5		
Coefficients (kPa)	Min	Mid	Max	0 NIHU	5 NIHU	10 NIHU	0 NIHU	5 NIHU	10 NIHU
Clot samples									
a10	− 5.99	− 0.74	− 6.15	− 5.69	− 0.51	− 1.21	2.61	8.37	0.545
a01	6.29	1.01	6.54	6.05	0.69	1.45	− 2.45	− 8.35	− 0.09
a20	− 70.61	− 6.33	− 14.96	− 14.17	− 4.90	− 5.84	1.91	11.54	− 9.33
a11	88.57	9.04	21.75	20.56	6.87	8.60	2.84	− 17.00	12.12
a30	17.89	1.32	1.68	1.61	1.09	1.16	0.07	− 0.58	2.03

	0 NIHU			Animal 3			Animal 5		
% strain	Min	Mid	Max	0 NIHU	5 NIHU	10 NIHU	0 NIHU	5 NIHU	10 NIHU
Young modulus (kPa)									
5	0.12	1.53	1.70	0.31	1.06	1.13	1.95	3.30	3.05
10	0.18	2.13	4.90	0.24	1.50	1.63	2.45	4.31	3.86
20	2.02	6.17	11.67	2.01	2.78	3.40	2.92	4.56	5.36
30	3.24	9.86	24.39	3.20	4.47	5.65	3.41	5.85	7.04
40	3.97	16.60	61.69	3.97	7.48	9.14	4.24	9.33	10.91
50	5.98	–	–	6.03	13.15	15.22	5.45	14.68	19.62
60	11.57	–	–	11.57	–	–	–	21.13	–
70	23.17	–	–	22.95	–	–	–	–	–

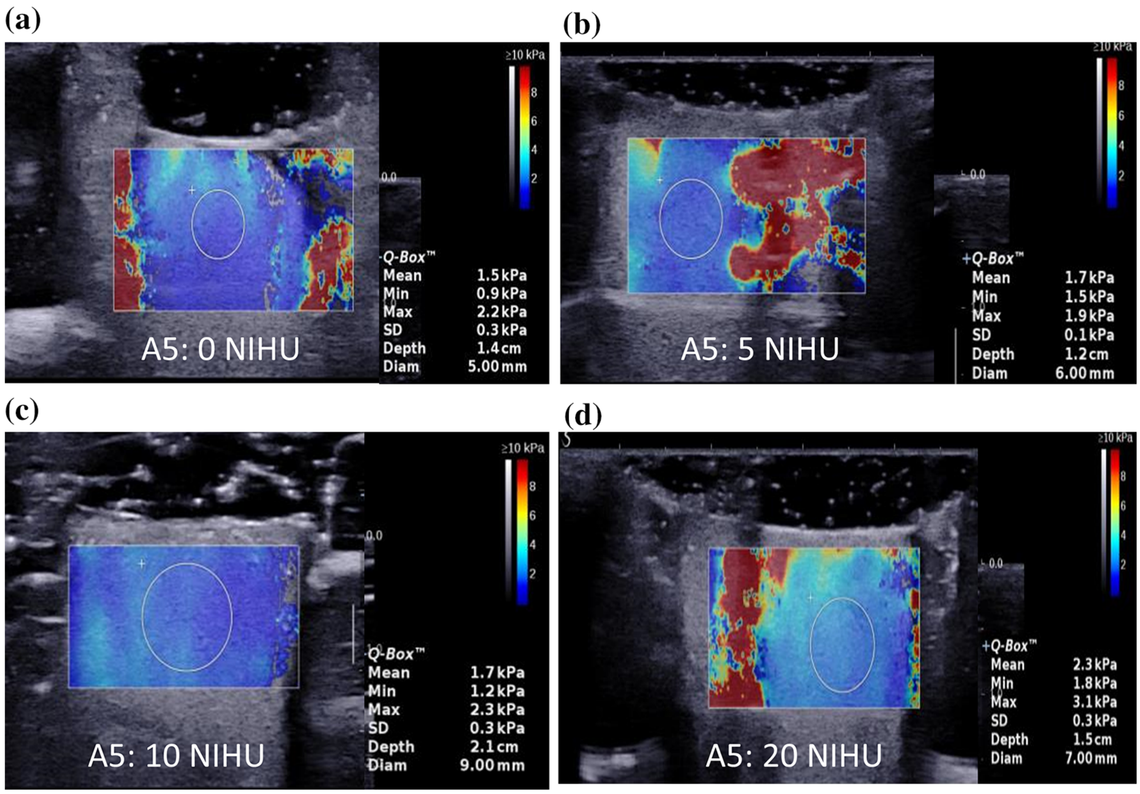

FIGURE 5. Regions of interest (circles) display the initial elastic modulus under Ultrasound Shear Wave Elastography in EAs with (a) no added thrombin; (b) 5 NIHU; C: 10 NIHU; D: 20 NIHU (Animal 5).

bin, the average Young modulus varied from 0.12 to 61.7 kPa for a percentage strain variation of 5 to 40%. The addition of 10 NIHU of thrombin increased the average stiffness for Animal 3 and Animal 5.

Ultrasound Shear Wave Elastography

Figures 5a–5d displays the elastic modulus along a 2D plane for four clot samples with thrombin concentrations varying from 0 to 20 NIHU of thrombin. The shear wave speed ranged from 0.68 to 0.85 m/s for the four clot samples. The initial elastic modulus measurements were made within the selected region of interest (ROI) (indicated by the circles in Fig. 5) and had mean values of 1.5–2.3 kPa and a range of 0.9–3.1 kPa. A 53% increase in the mean Young modulus was measured with an increase of thrombin from 0 to 20 NIHU. The measurement ROIs were positioned wholly within the region of the clot by an experienced user (AF) to ensure no contribution from the surrounding agar.

Parallel Plate Rheometry

Figures 6a and 6b show the storage (G'—solid line) and loss (G''—dashed line) moduli for three animals with no added thrombin (Fig. 5a) and one animal with added thrombin (Fig. 5b). Figures 6c and 6d show the absolute shear modulus value, $|G^*|$, for Figs. 6a and 6b, respectively. There was a non-linear viscoelastic response for both the storage and loss modulus for all strain values. With increasing strain there was a decrease and an increase in storage and loss modulus, respectively. When the ratio of storage to loss modulus equals one (phase angle of 45°) the sample turns into a liquid, marking the end of the test. For the three animal samples with no added thrombin, the maximum storage modulus varied from 0.04 to 0.13 kPa. The storage modulus peaked from 0.13 to 0.42 kPa with increasing thrombin concentration. There was an increase of 2% in the absolute shear modules value across all samples.

Indentation

Figure 7a shows the five positions for the indentation tests. Figures 7b and 7c show the load-extension for five 1 mm indentations on the top and bottom of one clot sample with no added thrombin. Elastic contact theory was used to estimate the elastic modulus based on these load-extension curves. The elastic modulus was calculated for a rigid cylindrical flat punch tip by the following formula[16] given by:

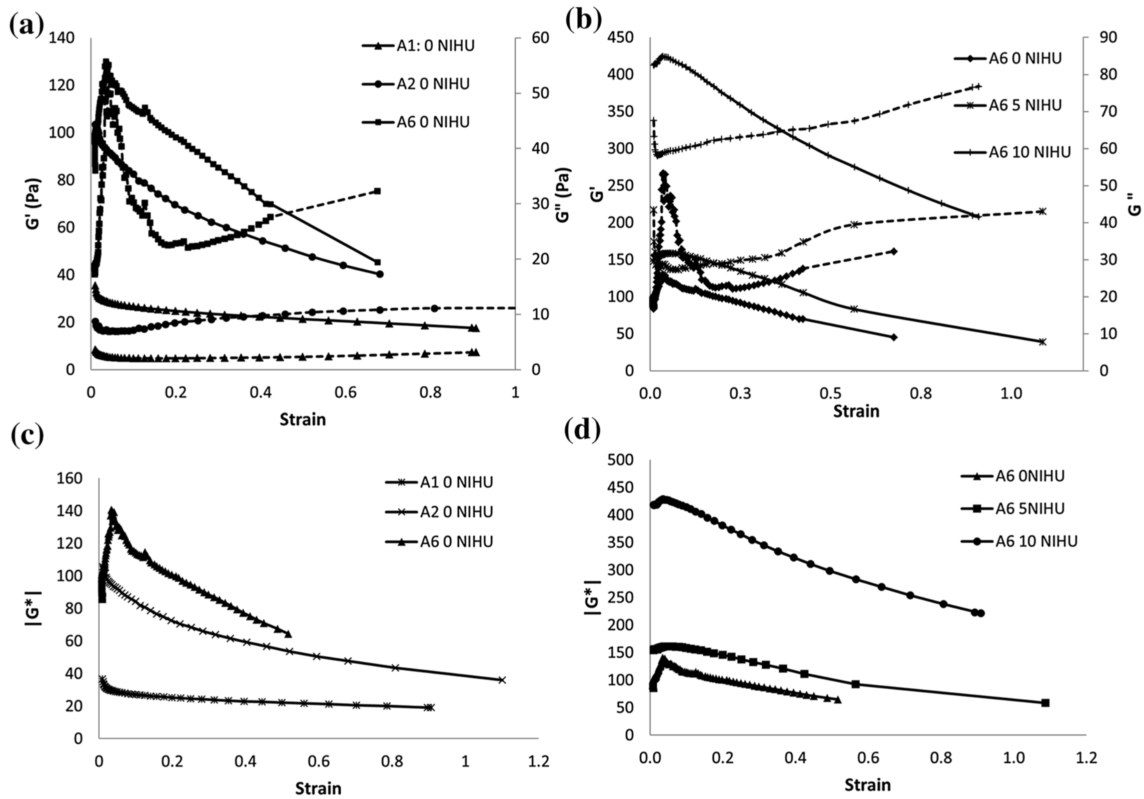

FIGURE 6. (a) Storage (G' - solid line) and loss (*G″*—dashed line) moduli for three cylindrical EAs from three different animals, with no added thrombin; (b) Storage (*G′*—solid line) and loss (*G″*—dashed line) moduli for three cylindrical EAs from same animal (Animal 6), with varying concentrations of thrombin; (c) Absolute shear modulus for three cylindrical EAs from three different animals, with no added thrombin; Absolute shear modulus for three EAs from same animal (Animal 6), with varying concentrations of thrombin added.

$$E(h) = \frac{3P(h)}{8rh} \tag{22}$$

where R is the punch radius, P is the load at indentation depth, and h is the instantaneous indentation depth. This equation assumes that the Poisson ratio, v, is equal to 0.5, which is a reasonable assumption for thrombi.[23] Figure 7d shows the boxplot for the E values for all 10 indentations. The median values varied from 1.58 kPa (top) to 1.80 kPa (bottom). There was no significant difference between the top and bottom (p value < 0.05) as found by the Mann–Whitney non-parametric 95% CI test.

Creep and Stress Relaxation

Figures 8a and 8b show the creep strain for 3 loads (0.3 N, 1 N, 2 N) and the stress relaxation at 3 displacements (1 mm, 2 mm, 4 mm), respectively with corresponding Standard Linear Solid (SLS) model. Table 4 displays the creep and stress relaxation best fit coefficients for the Standard Linear Solid model. Both samples were fabricated without thrombin.

DISCUSSION

As far as the authors are aware, this is the first study where bovine EAs, with and without the addition of thrombin, have been histologically and mechanically described under seven different loading conditions with corresponding proposed constitutive equations. Previous studies have tested EAs and/or human blood clots under one or two loading conditions (tensile,[21] compression,[6,8,21,26] elastography,[3,27,29] rheometry,[5] dynamic compression[29] and dynamic elastography[27]). However, none provided constitutive models for describing the non-linear stress–strain response of blood clots.

The bovine EAs displayed similar compositional structures to human specimens retrieved from stroke treatment procedures under H and E and MSB histology staining, which confirmed that bovine EAs are suitable for the mimicking cardiac source clots. In future studies, the presence of platelets should be addressed histologically using, for example, the Giemsa stain. The addition of thrombin was found to improve the specimen stability. It was observed that mam-

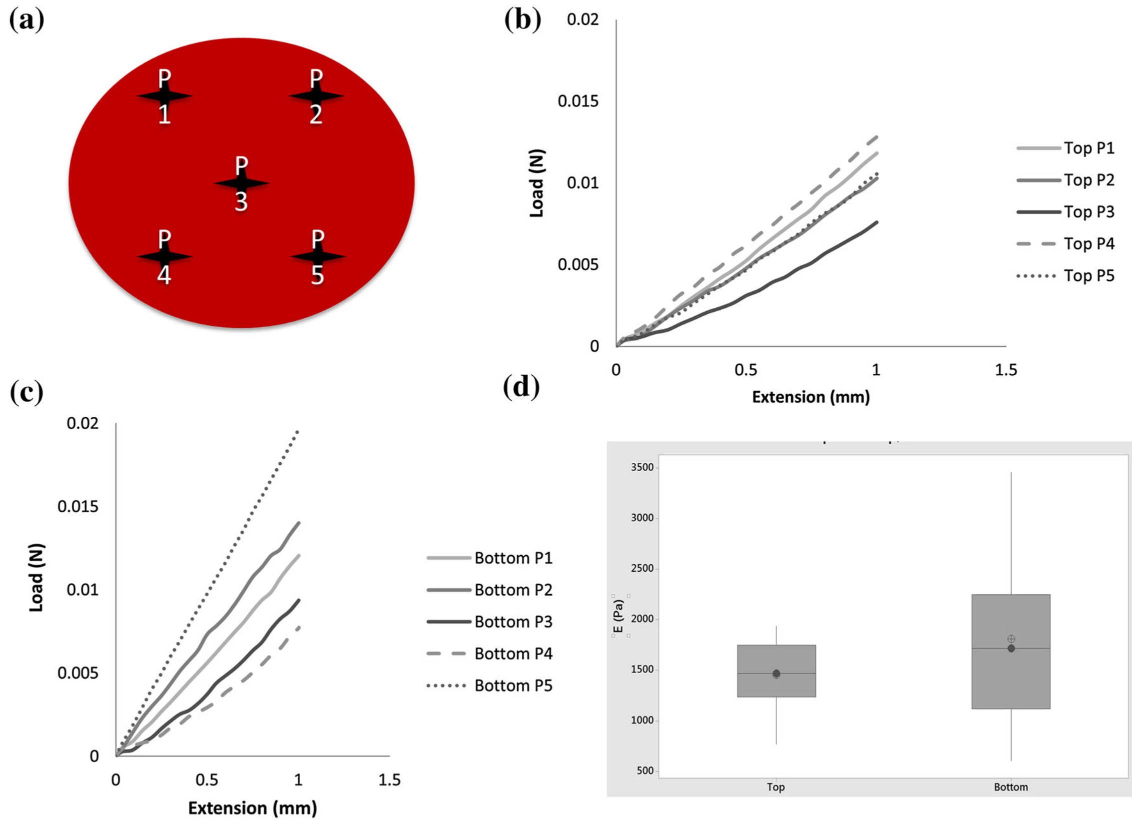

FIGURE 7. (a) Five positions for indentation tests; (b) Load-extension results for five indentations on the top of a cylindrical EA (Animal 4); (c) Load-extension results for five indentations on the bottom of the same cylindrical EA (Animal 4); (d) Boxplot for Young modulus for all 10 indentations.

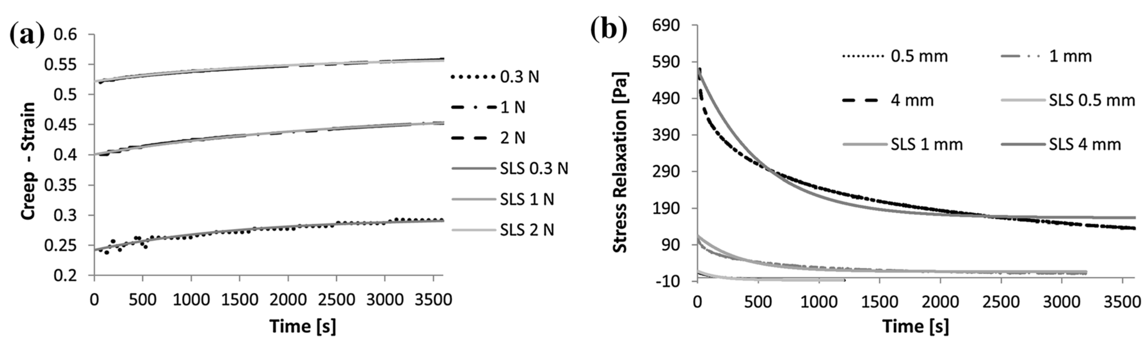

FIGURE 8. (a) Experiment Creep strain data for 3 loads (Dashed Line) on the same cylindrical EA (Animal 4), with corresponding SLS models (Solid Line); (b) Experimental stress relaxation at 3 displacements (Dashed Line) on the same cylindrical EA (Animal 5), with corresponding SLS models (Solid Line).

malian thrombi models induced with low concentrations of bovine thrombin had lower structural integrity than those induced with higher thrombin concentrations upon manual inspection.

The tensile results exhibited a linear stress–strain within 0–20% strain, with a Young modulus ranging from 14 to 50 kPa (Fig. 3a). This was higher than the tensile E value for porcine EAs tested by Krasokha *et al.*[21] with reported *E* values of 2–3.8 kPa at 300% elongation. This variation in results could be attributed to the difference in species tested and also to their use of cylindrical-dogbone samples of unspecified dimension. Of the 32 dogbone EA specimens fabricated for tensile testing in the current study, only four samples were successfully transferred from the mould and tested in tension. Three of these slipped at the clamps and one sample was successfully pulled to failure, showing two distinct linear regions, similar to arterial tissue, and fitted successfully with the 3rd order Mooney–Rivlin constitutive model. This difficulty in handling

TABLE 4. Creep and stress relaxation best fit coefficients for the standard linear solid model obtained from two blood clots with 0 NIH units.

	Creep			Stress relaxation		
Set-up	0.3 N	1 N	2 N	0.5 mm	1 mm	4 mm
Stress (Pa)	424	1415	2829	–	–	–
Strain	–	–	–	0.02	0.06	0.30
E_1 (Pa)	1752.09	3531.75	5420.59	735.53	2005.77	1923.43
E_2 (Pa)	7911.89	20765.40	71530.13	− 197.51	344.36	777.21
μ (Pa s)	12223093.59	51485720.86	127911898.19	90301.96	820019.89	1404786.42
τ (s)	1544.90	2479.40	1788.22	167.84	348.92	520.17

perhaps accounts for the limited reports of uniaxial tensile testing of blood EAs in literature. Hooks were also used in an attempt to prevent slipping of the sample; however this just resulted in ripping the sample. An adapted holder for the cylindrical component of the dogbone that could apply a uniform suction to the sample could improve gripping and minimise slippage.

Compression testing of EAs proved to be a less laborious task, with a greater sample size tested. There was a substantial variation in values (Figs. 5a–5c and Table 3) of 0–10 NIHU for 2 clot samples with variations in compressive Young modulus of 0.31–1.13 kPa and 1.95–3.30 kPa at 5% strain. All samples had a non-linear stress–strain response with further increases in Young modulus with increasing strain. The Mooney–Rivlin 3rd Order constitutive model was a suitable fit for the EAs under compression. The compression stress–strain curves and stiffness values are in agreement with those found for red emboli retrieved from human and porcine EAs.[6] Chueh *et al.*[6] also found an increase in compressive Young modulus with the addition of thrombin ($E_{0-75\%}$ = 50–70 kPa (5NIHU)), which was higher than the maximum Young modulus range for bovine EAs in our study. Chueh *et al.*[6] showed compressive Young modulus for bovine (50–70 kPa), porcine (45–60 kPa) and human (20 kPa) EAs. These EAs were initially treated with anticoagulant citrate dextrose to prevent instant coagulation. Coagulation was induced using thrombin and calcium chloride. This different sample preparation could explain the differences in Young modulus between those EAs and the EAs in this study. Here, the initial compressive Young modulus was determined using Shear Wave Elastography. For the same animal (A5), the results of the SWE were in agreement with the compression testing.

The indentation tests had a linear relationship of load vs. 1 mm extension. There was a variation in Young modulus, as derived from Eq. (15) of 1.28 kPa (Q1, top) to 2.95 kPa (Q4, bottom). This wide variation was in agreement with the compression results for four clots derived from the same animal (A4). Based on the Mann–Whitney 95% CI test, there was no significant difference ($p < 0.05$) between top and bottom surfaces, showing homogeneity of the clot. Future studies should include an investigation into the effects of the thrombin addition on the surface integrity of the clot samples. A greater sample size is also necessary.

There was a non-linear viscoelastic response for both the storage and loss moduli for all strain values. With increasing strain there was a decrease and an increase in storage and loss modulus, respectively. When the ratio of storage and loss modulus equals one (phase angle of 45°) the sample turns into a liquid, marking the end of the test. At very low strains, the storage modulus peaked from 0.13 to 0.42 kPa with increasing thrombin concentration. Schmitt *et al.*[27] measured the shear modulus of 9 porcine blood samples during the coagulation period after 16 h and reported a shear modulus of 0.900 ± 0.189 kPa. The shear modulus of the bovine EAs in this study lies within literature findings,[5,14] who found the torsional shear storage moduli to be 0.3 and 2.3 kPa, respectively. The shear modulus found by Carr *et al.*[5] is higher than our results as these were for diabetic patients with a high platelet count.

There are very limited time-dependant tests available in literature. Chueh *et al.*[6] performed compressive stress relaxation tests on EAs for 5 min and upon removal of the load, accessed strain recovery; however, their study did not report on the varying stress values during testing. This study seems to be the first time that three different loading and displacement conditions were applied for creep and stress relaxation tests, respectively. The non-linear viscoelastic response of the EAs were displayed by creep and relaxation test results. The SLS model was an excellent fit for the creep data and proved to be a good trend for the stress relaxation data. The relaxation time, as presented in Table 4, was recorded as the time taken to reach 63% of its equilibrium time. The creep and stress relaxation tests recorded relaxation times of 1545–2489 s and 168–520 s, respectively. There was a percentage increase in strain and percentage decrease in stress of

6.5–20.2% and 76–140%, respectively, over the 1 h period. Further studies are required on a larger sample size with the addition of thrombin for a longer period of time to assess the effect of thrombin on creep and stress relaxation.

There were several limitations to this study. Only one species was used in the fabrication of the EAs. While other studies have confirmed the suitability of bovine EAs as human blood analogues,[6] a valuable study may include fabrication of porcine and ovine derived EAs for comparison against the bovine EAs. The mechanism of coagulation is universal across mammalian biology, including human biology[7] and thus varieties of mammalian blood should be investigated for further EA fabrication. Red blood cell rich clots associated with spontaneous coagulation were tested. While these clot types are suitable for cardiac sourced clot replication, an array of clot types, ranging from soft red emboli to hard atherosclerotic plaque, emboli have been withdrawn from stroke patients.[6] These variations in clot types should be mimicked and mechanically compared with the bovine EAs fabricated in this study. It would be best to fabricate all samples from the same animal; however the volume of blood required does not permit this. All clots discussed in this work have ranged in age from 1 to 3 days. The natural ageing effect on a blood clot has not been examined, which could alter clot composition and thus mechanical behaviour.

Overall, this project has quantified the major mechanical properties of bovine EAs, with and without the addition of thrombin. The mechanical characterisation of EAs is an important element for preclinical evaluation of thrombectomy devices.

CONCLUSION

These bovine EAs histologically reflect the appearance of human emboli. The EAs display similar mechanical characteristics to other EAs reported in literature as well as emboli retrieved from AIS patients. The addition of thrombin increased the stiffness of the EAs and improved observed structural integrity. There was quite a large variation in the mechanical characteristics of the bovine EAs, even for clots derived from the same animal. This shows the natural variation that can occur with biological samples. The 3rd order Mooney–Rivlin constitutive equation and Standard Linear Solid model satisfactorily fit the non-linear stress–strain response and time-dependent properties, respectively. These equations and experimental data can be applied for future numerical and experimental testing.

FUNDING

Galway Mayo Institute of Technology 40th Anniversary Seed Funding.

CONFLICT OF INTEREST

All authors declare that they have no conflicts of interest.

ETHICAL APPROVAL

All applicable international, national, and/or institutional guidelines for the care and use of animals were followed. Burkes Ltd., is an EU approved abattoir. This article does not contain any studies with human participants performed by any of the authors.

REFERENCES

[1] Beldi, G., L. Beng, G. Siegel, S. Bisch-Knaden, and D. Candinas. Prevention of perioperative thromboembolism in patients with atrial fibrillation. *Br. J. Surg. Nov.* 94(11):1351–1355, 2007.

[2] Bernal, M., F. Chammings, M. Couade, J. Bercoff, M. Tanter, and J. L. Gennisson. In vivo quantification of the nonlinear shear modulus in breast lesions: feasibility study. *IEEE Trans. Ultrason. Ferroelectr. Frequ. Control* 63(1):101–109, 2016.

[3] Brophy, D. F., R. J. Martin, T. W. Gehr, and M. E. Carr. A hypothesis-generating study to evaluate platelet activity in diabetics with chronic kidney disease. *Thromb. J.* 3(1):3, 2005.

[4] Campbell, W. B., B. M. Ridler, and T. H. Szymanska. Two-year follow-up after acute thromboembolic limb ischaemia: the importance of anticoagulation. *Eur. J. Vasc. Endovasc. Surg.* 19:169–173, 2000.

[5] Carr, M. E., A. Krishnaswami, and E. J. Martin. Platelet contractile force (PCF) and clot elastic modulus (CEM) are elevated in diabetic patients with chest pain. *Diabet. Med.* 19(10):862–866, 2002.

[6] Chueh, J. K., A. K. Wakhloo, G. H. Hendricks, C. F. Silva, J. P. Weaver, and M. J. Gounis. Mechanical characterisation of Thromboemboli in acute ischemic stroke and Laboratory Embolus Analogues. *Am. J. Neuroradiol.* 32:1237–1244, 2011.

[7] Davie, E. W., and K. Fujikawa. Basic mechanisms in blood coagulation. *Annu. Rev. Biochem.* 44:799–829, 1975.

[8] Dempfle, C. E., T. Kalsch, E. Elmas, N. Suvajac, T. Luecke, E. Muench, and M. Borggrefe. Impact of fibrinogen concentration in severely ill patients on mechanical properties of whole blood clots. *Blood Coagul Fibrinolysis* 19:765–770, 2008.

[9] Eggebrecht, H., A. Schmermund, T. Voigtländer, P. Kahlert, R. Erbel, and R. H. Mehta. Risk of stroke after transcatheter aortic valve implantation (TAVI): a meta-analysis of 10,037 published patients. *EuroIntervention* 8:129–138, 2012.

[10]Fuster, V., L. E. Ryden, D. S. Cannom, H. J. Crijns, A. B. Curtis, K. A. Ellenbogen, J. L. Halperin, J. Y. Le Heuzey, G. N. Kay, J. E. Lowe, S. B. Olsson, E. N. Prystowsky, J. L. Tamargo, S. Wann, S. C. Smith, Jr, A. K. Jacobs, C. D. Adams, J. L. Anderson, E. M. Antman, J. L. Halperin, S. A. Hunt, R. Nishimura, J. P. Ornato, R. L. Page, B. Riegel, S. G. Priori, J. J. Blanc, A. Budaj, A. J. Camm, V. Dean, J. W. Deckers, C. Despres, K. Dickstein, J. Lekakis, K. McGregor, M. Metra, J. Morais, A. Osterspey, J. L. Tamargo, and J. L. Zamorano. Guidelines for the management of patients with atrial fibrillation. *Circulation* 114:257–354, 2006.

[11]Gennisson, J. L., M. Renier, S. Catheline, C. Barriere, J. Bercoff, M. Tanter, and M. Fink. Acoustoelasticity in soft solds: assessment of the non-linear shear modulus with acoustic radiation force. *J. Acoust. Soc. Am.* 122(6):3211–3219, 2007.

[12]Gralla, J., G. Schroth, L. Remonda, A. Fleischmann, J. Fandino, J. Slotboom, and C. Brekenfeld. A dedicated animal model for mechanical thrombectomy in acute Stroke. *AJNR* 27:1357–1361, 2006.

[13]Heeringa, J., D. A. van der Kuip, A. Hofman, J. A. Kors, G. van Herpen, B. H. Stricker, T. Stijnen, G. Y. Lip, and J. C. Witteman. Prevalence, incidence and lifetime risk of atrial fibrillation: the Rotterdam study. *Eur. Heart. J.* 27:949–953, 2006.

[14]Isogai, Y., A. Iida, I. Chikatsu, K. Mochizuki, and M. Abe. Dynamic viscoelasticity of blood during clotting in health and disease. *Biorheology* 10(3):411–424, 1973.

[15]Jiang, Y., L. Guoyang, L. X. Qian, S. Liang, M. Destrade, and Y. Cao. Measuring the linear and non linear elastic properties of brain tissue with shear waves and inverse analysis. *Biomech. Model Mechanobiol.* 14:1119–1128, 2014.

[16]Juliano, T. F., A. M. Forster, P. L. Drzal, T. Weerasooriya, P. Moy, and M. R. VanLandingham. Multiscale mechanical characterization of biomimetic physically associating gels. *J. Mater. Res.* 21(8):2084–2092, 2006.

[17]Kan, I., I. Yuki, Y. Murayama, F. A. Vinuela, R. H. Kim, H. V. Vinters, and F. Vinuela. A novel method of thrombus preparation for use in a swine model for evaluation of thrombectomy devices. *AJNR* 31:1741–1743, 2010.

[18]Kannel, W. B., and E. J. Benjamin. Status of the epidemiology of atrial fibrillation. *Med. Clin. N. Am.* 92:17–40, 2008.

[19]Kay, R., J. Woo, L. Kreel, H. Y. Wong, R. Teoh, and M. G. Nicholls. Stroke subtypes among Chinese living in Hong Kong: the Shatin Stroke Registry. *Neurology*. 42:985–987, 1992.

[20]Kline, J. A., and R. S. Runyon. Pulmonary embolism and deep vein thrombosis. In: Emergency Medicine Concepts and Clinical Practice7th, edited by J. A. Marx, R. S. Hockberger, and R. M. Walls. New York: Elsevier, 2010, pp. 1157–1169.

[21]Krasokha, N., W. Theisen, S. Reese, P. Mordasini, C. Brekenfeld, J. Gralla, J. Slotboom, G. Schrott, and H. Monstadt. Mechanical properties of blood clots—a new test method. *Mat wiss u Werkstofftech*. 41:1019–1024, 2010.

[22]Lalley, C., A. J. Reid, and P. J. Prendergast. Elastic behaviour of porcine coronary artery tissue under uniaxial and equibiaxial tension. *Ann. Biomed. Eng.* 32(10):1355–1364, 2004.

[23]Maier, A., M. W. Gee, C. Reeps, H.-H. Eckstein, and W. A. Wall. Impact of calcifications on patient-specific wall stress analysis of abdominal aortic aneurysms. *Biomech. Model. Mechanobiol.* 9:511–521, 2010.

[24]Menke, J., L. Lüthje, A. Kastrup, and J. Larsen. Thromboembolism in atrial fibrillation. *Am. J. Cardiol.* 105:502–510, 2010.

[25]Prystowsky, E. N. The history of atrial fibrillation: the last 100 years. *J. Cardiovasc. Electrophysiol.* 19:575–582, 2008.

[26]Robinson, R. A., L. H. Herbertson, S. Sarkar Das, R. A. Malinauskas, W. F. Pritchard, and L. W. Grossman. Limitations of using synthetic blood clots for measuring in vitro clot capture efficiency of inferior vena cava filters. *Med. Dev. (Auckland, N.Z.)* 6:49–57, 2013.

[27]Schmitt, C., A. H. Henni, and G. Cloutier. Characterization of blood clot viscoelasticity by dynamic ultrasound elastography and modeling of the rheological behaviour. *J. Biomech.* 44:622–629, 2011.

[28]Sigrist, R. M. S., J. Liau, A. El Kaffas, M. C. Chammas, and J. K. Willmann. Ultrasound elastography: reviwe of techniques and clinical applications. *Theranostics* 7(5):1303, 2017.

[29]Whitbourne, P. G. S. Changes in the Clotting Viscoelasticity Caused by Cardiopulmonary Bypass (CPB) Surgery [dissertation]. MA: Cambridge Massachusetts Institute of Technology, 1998.